IEEE Access
Multidisciplinary : Rapid Review : Open Access Journal

Received 30 December 2022, accepted 7 January 2023, date of publication 10 January 2023, date of current version 19 January 2023.

Digital Object Identifier 10.1109/ACCESS.2023.3235885

RESEARCH ARTICLE

A Novel Control Strategy for Uninterruptible Power Supply Based on Backstepping and Fuzzy Neural Network

YANFEI DONG, GUOYONG ZHANG, GUOFENG HE, AND WENJIE SI
School of Electrical and Control Engineering, Henan University of Urban Construction, Pingdingshan 467036, China
College of Electrical Engineering and New Energy, China Three Gorges University, Yichang 443002, China

Corresponding author: Guofeng He (dragonhgf@hncj.edu.cn)

This work was supported by the Natural Science Fund Project of Henan Province, China, under Grant 222300420400.

ABSTRACT This paper proposes a novel control strategy for controlling the uninterruptible power supply (UPS) inverter, which is based on backstepping control theory combined with a fuzzy neural network (FNN). The advantage of backstepping control is that it can decompose a complex system into multiple subsystems, stabilize the control object according to Lyapunov stability theory, and simplify the controller design. However, it requires prior knowledge of multiple system parameters. FNN can approximate arbitrary nonlinear functions and system errors, which can reduce the parameters required for controller design. Hence, Combining the advantages of both methods, a UPS inverter control method with only a few parameters is designed. Then the sliding mode gain is added to compensate for the fuzzy neural network to reduce the chattering when the system operates and ensure the needed power quality. To verify the effectiveness of the proposed control system, the effectiveness of the proposed method is verified by a simulation experiment platform.

INDEX TERMS Power quality, fuzzy neural network (FNN), backstepping control, uninterruptible power supply (UPS).

I. INTRODUCTION

Uninterruptible Power Supply (UPS) is used to provide continuous, stable, and uninterrupted energy to critical equipment. With the rapid development of digital technology and communication technology, critical power consumption equipment customers have put forward a more stringent demand for power quality, and the demand for UPS is growing rapidly. UPS has been widely used to reduce economic losses caused by power outages [1], [2].

The online UPS [3] inverter is constantly at work and only switches to bypass mode when the inverter fails. When the grid fails, the storage unit, such as batteries, is switched to provide energy to the inverter, making for uninterrupted output voltage and suppressing spikes, surges, and frequency drift. Compared to the backup UPS [4] and online interactive UPS [5], the online UPS has been more widely used. The approach in this paper is based on the online UPS system and its general diagram is shown in Fig. 1.

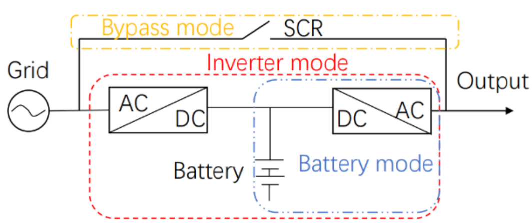

FIGURE 1. Online UPS working mode.

When the utility power is working normally, UPS works in inverter mode, converting AC to DC through rectification and power factor correction sections, which as battery charging power and inverter DC power. Once the utility failure is detected, the battery discharges as a DC power supply to the

The associate editor coordinating the review of this manuscript and approving it for publication was Norbert Herencsar.

inverter. The microprocessor detects a UPS failure and opens the bypass switch to operate in bypass mode.

The existing inverter UPS control methods are mainly virtual synchronous generator (VSG) [6], [7] and droop control [8], [9]. Meng et al. based on the comparison of conventional sag control and VSG control proposed generalized droop control (GDC) for grid-supported inverters is presented [10]. The backstepping controller and FNN have excellent performance in complex nonlinear systems, but their application on UPS needs to be further explored.

The backstepping controller transforms a complex nonlinear system into multiple subsystems, stabilizing all of the subsystems from back to front. The authors provide sinusoidal voltages with low harmonic distortion through adaptive backstepping control for UPS systems [11]. Katir et al. designed a backstepping controller to control N-cascaded H-bridge multilevel inverter [12]. Wang and Wai studied the design of a discrete-time backstepping sliding mode control (DTB-SMC) method for LCL-type grid-connected inverters [13]. Ali et al. applied backstepping control to PV maximum power point tracking(MPPT) and showed good response speed and steady-state results [14].

Yang and Ye used nonsingular fixed-time fault-tolerant fuzzy control for nonlinear systems [15]. The authors used finite-time adaptive neural networks to implement tracking problems for nonlinear quantized systems [16], coping with limited-time quantitative feedback control problems. The fuzzy neural network(FNN) is essentially a neural network with fuzzy signals and fuzzy weights input to a conventional one. Its structure is like a neural network, and its function is a fuzzy system. It has a stronger knowledge representation capability than neural networks and overcomes the dependence on expert knowledge for fuzzy system rule design. By adjusting the weights, FNN can achieve an approximation of arbitrary nonlinear functions. Xu et al. used a fuzzy PID approach to improve power quality in UPS inverter circuits [17]. The authors used fuzzy models to obtain quantitative estimates of environmental initiation projects in air transportation [18]. The authors implement supervised fuzzy neural network control (SFNNC) to control the three-phase inverter of a UPS [19]. Zheng et al. used FNN to solve control problems for complex robotic systems with uncertainty and disturbances [20]. Ascensão et al. Applied fuzzy logic to medical treatment of autism [22].

To solve the problems of UPS parameters and disturbance uncertainty, a UPS system under adaptive backstepping sliding mode fuzzy neural network control is proposed. Firstly, the backstepping control is used to establish an initial UPS control system, and then sliding mode gain is added to enhance the robustness of the system. Finally, unknown device parameters and perturbations are approximated by a fuzzy neural network. The proposed UPS control system has the following characteristics:

1) The fuzzy neural system combines the feature of fuzzy logic and neural networks to approximate unknown parameters, and the control system design requires only the output voltage parameter.
2) The UPS system is transformed into two subsystems and the controller design without coordinate transformations. Combining the fuzzy system with the backstepping control, the self-learning capability of the neural network is introduced to reduce the fuzzy rule design in the FNN.

II. DYNAMIC MODEL OF UPS INVERTER

For UPS, especially the online UPS, the structure is shown in Fig. 2. It usually consists of the following components: the AC grid used to supply energy to the UPS, the power factor correction (PFC) circuit to convert AC to DC, the bypass system consisting of silicon controlled rectification (SCR), the inverter and filter circuit.

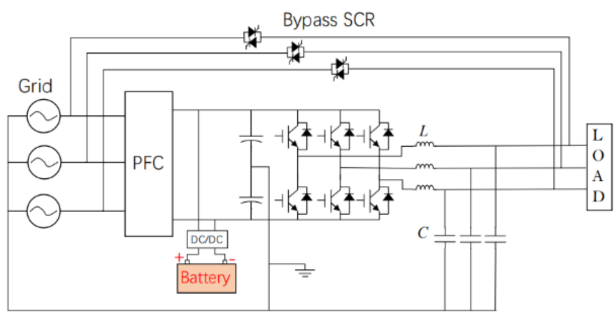

FIGURE 2. Online UPS working mode.

To represent the IGBT switching state, define the switching function

$$s_k = \begin{cases} 1 & \text{if } S_k \text{ is On and } S_{k+3} \text{ is Off} \\ 0 & \text{if } S_k \text{ is Off and } S_{k+3} \text{ is On} \end{cases}$$

where $k = 1, 2, 3$. Therefore $e_j = s_k V_{dc}$, where $j = a, b, c$. Without consideration of the energy transmission losses, according to Kirchhoff's law, the relationship between voltage and current can be obtained as

$$\begin{cases} L\dfrac{di_{La}}{dt} = e_a - u_a = s_1 V_{dc} - u_a \\ L\dfrac{di_{Lb}}{dt} = e_b - u_b = s_2 V_{dc} - u_b \\ L\dfrac{di_{Lc}}{dt} = e_c - u_c == s_3 V_{dc} - u_c \end{cases} \tag{1}$$

$$\begin{cases} C\dfrac{du_a}{dt} = i_{La} - i_a \\ C\dfrac{du_b}{dt} = i_{Lb} - i_b \\ C\dfrac{du_c}{dt} = i_{Lc} - i_c \end{cases} \tag{2}$$

For easy description, equations (1) and (2) are rewritten as

$$\dot{i}_{Lj} = s_k \frac{V_{dc}}{L} - \frac{u_j}{L} \tag{3}$$

$$\dot{u}_j = \frac{i_{Lj}}{C} - \frac{i_j}{C} \tag{4}$$

Derivation of equation (4) yields

$$\begin{aligned}\ddot{u}_j &= \frac{1}{C}(s_k\frac{V_{dc}}{L} - \frac{u_j}{L}) - \frac{1}{C}\dot{i}_j \\ &= s_k\frac{V_{dc}}{CL} - \frac{u_j}{CL} - \frac{\dot{i}_j}{C} \\ &= g(u_j, i_j) + bu \end{aligned} \tag{5}$$

where $g(u_j, i_j) = -\frac{u_j}{CL} - \frac{\dot{i}_j}{C}$, $u = s_k$, $b = \frac{V_{dc}}{CL}$.

Considering the sensor measurement errors and external environmental disturbances, the UPS inverter dynamic model can be described as

$$\begin{aligned}\ddot{u}_j &= g(u_j, i_j) + bu + f_d \\ &= f + bu \end{aligned} \tag{6}$$

where $f = g(u_j, i_j) + f_d$. The dynamic perturbation f_d is a bounded unknown variable, satisfying $0 \le f_d < M$, M is a constant value.

III. THE PROPOSED CONTROL STRATEGY

Based on the mathematical model of the UPS, this section designs the backstepping control method. Using virtual and actual control quantities, the whole UPS system is gradually stabilized and able to track the target value.

First, according to the objective function, the tracking error is defined as

$$z_1 = u_j - z_d \tag{7}$$

where z_d is the reference voltage, u_j is the output voltage feedback value measured by sensors.

Design a virtual control function as

$$\alpha_1 = -c_1 z_1 + \dot{z}_d \tag{8}$$

where c_1 is a positive constant.

Design a *Lyapunov* function as

$$V_1 = \frac{1}{2}z_1^2 \tag{9}$$

Then

$$\dot{V}_1 = z_1\left(\dot{u}_j - \dot{z}_d\right) \tag{10}$$

Define the error function as

$$z_2 = \dot{u}_j - \alpha_1 \tag{11}$$

Substituting (11) into (10), we get

$$\begin{aligned}\dot{V}_1 &= z_1\left(z_2 + \alpha_1 - \dot{z}_d\right) \\ &= z_1\left(-c_1 z_1 + z_2\right) \\ &= -c_1 z_1^2 + z_1 z_2 \end{aligned} \tag{12}$$

If $z_2 = 0$, there is $\dot{V}_1 = -c_1 z_1 < 0$.

To improve the robustness of the control system, define a sliding mode surface

$$s = z_2 \tag{13}$$

Deriving equation (13)

$$\begin{aligned}\dot{z}_2 &= \ddot{u}_j - \dot{\alpha}_1 \\ &= f + bu + c_1\dot{z}_1 - \ddot{z}_d \end{aligned} \tag{14}$$

Design the second *Lyapunov* function as

$$V_2 = V_1 + \frac{1}{2}z_2^2 \tag{15}$$

Then

$$\begin{aligned}\dot{V}_2 = &-c_1 z_1^2 + z_1 z_2 \\ &+ z_2\left(f + bu + c_1\dot{z}_1 - \ddot{z}_d\right) \end{aligned} \tag{16}$$

According to (16), the backstepping control law is designed as

$$\begin{aligned}u = \frac{1}{b}(&-f - c_1\dot{z}_1 + \ddot{z}_d \\ &- z_1 - c_2 z_2 - \eta\,\mathrm{sgn}\,(s)) \end{aligned} \tag{17}$$

To enhance the robustness of the controller and improve the anti-interference capability, the switching term $\eta\mathrm{sgn}(s)$ is introduced. Where c_2, η are two positive constants, sgn is a symbolic function. In the control law (17), two derivatives terms and a switching term are included. The control law will be limited to the range of -1 to $+1$ during the inverter work and will be executed by the IGBT module after modulation.

Substituting (17) into (16)

$$\dot{V}_2 = -c_1 z_1^2 - c_2 z_2^2 - \eta|z_2| \le 0 \tag{18}$$

Since $\dot{V}_2 \le 0$, $\dot{V}_2$ is semi-negative definite, the system is asymptotically stable and the errors z_2 and z_1 will approach 0 at infinity. However, due to sensor measurement errors, device aging, and the presence of some unknown parameters, the function f is unknown, which results in the control law (17) not being directly available. Obtaining these difficult-to-measure parameters through observers or neural networks is a popular approach.

Due to the all-purpose approximation property of fuzzy neural networks for nonlinear functions and the simplicity of the design for easy operation, fuzzy neural networks are designed to estimate unknown functions f.

When approximating the unknown function by FNN, it can be adaptively adjusted by calculating the *Lyapunov* function. The measure can replace the empirical part of the fuzzy process. The general structure of a fuzzy neural network is shown in Fig.4. The four-layer network with the input layer, fuzzification layer, rule layer, and output layer is its basic structure, which corresponds to the following uses.

In the input layer, the neurons only introduce external inputs into the network without any algebraic processing and the number of nodes $N_1 = n$.

In the fuzzification layer, each node represents a membership function and calculates the index of affiliation belonging to each linguistic variable. These language variables

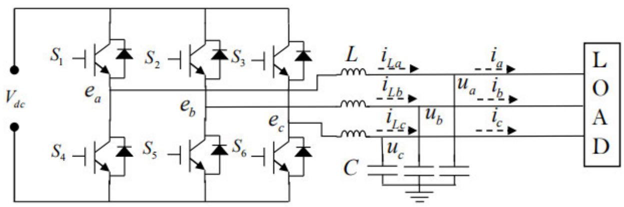

FIGURE 3. UPS inverter topology.

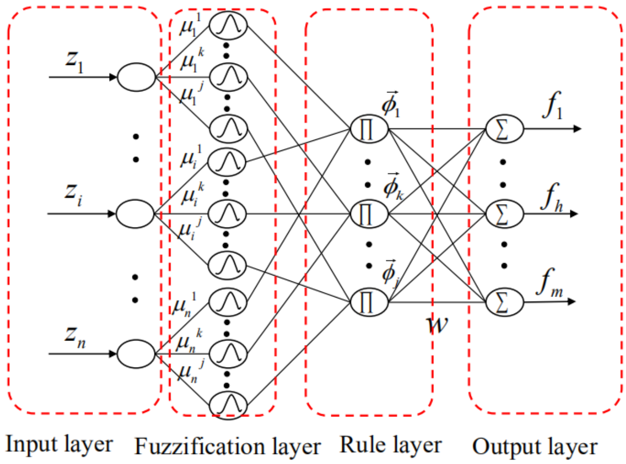

FIGURE 4. FNN basic structure.

will be used as input for the next layer. Such as the Gaussian function

$$\mu_i^j = \exp\left(-\frac{(z_i - c_{ij})^2}{\sigma_{ij}^2}\right) \tag{19}$$

where c_{ij} and σ_{ij} denote the center and width of the Gaussian membership function, respectively, and the total number of nodes in the layer $N_2 = jn$.

In the rule layer, each neuron represents a fuzzy rule and performs the 'and' operation, if the product is used to replace the take small operation

$$\vec{\phi}_j = \prod_{j=1}^{M} \mu_i^j \tag{20}$$

where $M = \prod_{i=1}^{n} M_i$, M_i is the ith fuzzification node, and the number of nodes $N_3 = j$.

In the output layer

$$f_l = \frac{\sum_{j=1}^{N} \psi_{lj}\bar{\phi}_j}{\sum_{j=1}^{N} \bar{\phi}_j} = \sum\nolimits_{j=1}^{N} \psi_{lj}\phi_j \tag{21}$$

where $l = 1, 2, \ldots, m$, the number of nodes in this layer $N_4 = m$

The mathematical model of the FNN can be expressed as

$$\tilde{f}_l = \psi^T \phi \tag{22}$$

where $\psi = [\psi_{l1}, \psi_{l2}, \ldots, \psi_{lj}]^T$, $\phi = [\phi_1, \phi_2, \ldots, \phi_j]^T$

The UPS inverter's unknown function f is described as follows by using FNN

$$f = \psi^{*T}\phi + \varepsilon \tag{23}$$

where ψ^{*T} is the optimal weight in the FNN approximation process, ε is the approximation error, satisfying $|\varepsilon| \le \varepsilon'$, and ε' is a small positive constant.

Design the third *Lyapunov* function

$$V_3 = V_2 + \frac{1}{2\eta}(\psi - \psi^*)^T(\psi - \psi^*) \tag{24}$$

Differentiation of the above equation

$$\dot{V}_3 = \dot{V}_2 + \frac{1}{2\eta}\left(\dot{\psi}^T\psi - \dot{\psi}^T\psi^* + \psi^T\dot{\psi} - \psi^{*T}\dot{\psi}\right) \tag{25}$$

Since ψ is a column vector, we can get $\dot{\psi}^T\psi = \psi^T\dot{\psi}$ and $\dot{\psi}^T\psi^* = \psi^{*T}\dot{\psi}$. Substituting (16) into (25), we get

$$\begin{aligned}\dot{V}_3 &= -c_1 z_1^2 + z_2(z_1 + f + bu + c_1\dot{z}_1 - \ddot{z}_d) \\ &\quad + \frac{1}{\eta}(\psi - \psi^*)^T\dot{\psi}\end{aligned} \tag{26}$$

Approximating the unknown function f by FNN, we can get a new control law

$$u = \frac{1}{b}\left(-\tilde{f} - c_1\dot{z}_1 + \ddot{z}_d - z_1 - c_2 z_2 - \eta\,\mathrm{sgn}(s)\right) \tag{27}$$

Substituting (27) into (26)

$$\begin{aligned}\dot{V}_3 &= -c_1 z_1^2 + z_2\left(f - \tilde{f} - c_2 z_2 - \eta\,\mathrm{sgn}(s)\right) \\ &\quad + \frac{1}{\eta}(\psi - \psi^*)^T\dot{\psi} \\ &= -c_1 z_1^2 - c_2 z_2^2 - \eta z_2\,\mathrm{sgn}(s) + z_2\left(f - \tilde{f}\right) \\ &\quad + \frac{1}{\eta}(\psi - \psi^*)^T\dot{\psi} \\ &= -c_1 z_1^2 - c_2 z_2^2 + z_2\left(\psi^{*T}\phi + \varepsilon - \psi^T\phi\right) \\ &\quad + \frac{1}{\eta}(\psi - \psi^*)^T\dot{\psi} - \eta z_2\,\mathrm{sgn}(s)\end{aligned} \tag{28}$$

Then

$$\begin{aligned}\dot{V}_3 &= -c_1 z_1^2 - c_2 z_1^2 - \eta|z_2| + z_2\varepsilon \\ &\quad - z_2(\psi - \psi^*)^T\phi + \frac{1}{\eta}(\psi - \psi^*)^T\dot{\psi}\end{aligned} \tag{29}$$

The adaptive weights of the fuzzy neural network are chosen as

$$\dot{\psi} = z_2\eta\phi \tag{30}$$

Equation (29) can be written as

$$\begin{aligned}\dot{V}_3 &= -c_1 z_1^2 - c_2 z_2^2 - \eta|z_2| + z_2\varepsilon \\ &\le -c_1 z_1^2 - c_2 z_2^2 - |z_2|(\eta - \varepsilon')\end{aligned} \tag{31}$$

If we choose $\eta \ge \varepsilon'$

$$\dot{V}_3 \le -c_1 z_1^2 - c_2 z_2^2 \le 0 \tag{32}$$

Define a function $g(t)$

$$\dot{V}_3 \leq -g(t) = -\left(c_1 z_1^2 + c_2 z_2^2\right) \tag{33}$$

Therefore

$$g(t) \geq 0 \tag{34}$$

$$\dot{g}(t) = 2c_1 z_1 \dot{z}_1 + 2c_2 z_2 \dot{z}_2 \tag{35}$$

where $\dot{g}(t)$is a bounded function, and the definition of V_3 shows that $V_3 \geq 0$. According to $Lyapunov - like$Lemma, $\lim_{t\to\infty} g(t) = 0$. Since c_1, c_2 are positive constants, the system is asymptotically stable.

The UPS inverter section has the following control topology as in Fig. 5

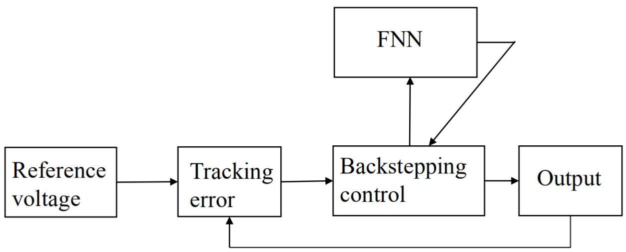

FIGURE 5. UPS inverter control topology.

IV. SIMULATION AND EXPERIMENTAL RESULTS

A. SIMULATION

The effectiveness of the proposed control strategy is verified in Matlab/Simulink. The UPS-related parameters are shown in Table.1.

TABLE 1. Simulation and experimental parameters.

DC voltage	500V
Filter Inductors	300uH
Filter capacitors	35uF
Switching frequency	10kHz
Output Reference Voltage	220V
Output voltage frequency	50Hz

In the fuzzy neural network, Gaussian functions are chosen as the membership functions with the general format$\mu = \exp[-((x+15)-5(i-1)/5)^2]$. Where $i = 1, 2, \ldots 7$. Control parameters c_1 =5000, c_2 =5000, η =100000, the initial weight of FNN is set to 0.

Nonlinear loads belonging to a general one, due to their characteristics, can easily cause a large impact on the output voltage and its hardware facilities when they are connected to the UPS. Experiments are conducted to verify the dynamic performance of the proposed control strategy when the rectifying loads are switched on at 0.05s moment and switched off at 0.1s in Matlab/Simulink. Where $R = 50\Omega, C = 20\mu F, L = 13mH$.

Fig.6 and Fig.7 represent the voltage and current waveforms under the proposed control method and the conventional controller from top to bottom. The proposed control strategy and the conventional strategy both achieve the target voltage within one cycle. But in the early stage of the system, the waveform under the proposed control strategy has fewer fluctuations and faster achievement of target values. This is due to the addition of a sliding mode gain to the conventional control strategy, which enhances system robustness while reducing system turbulence. After the system reaches the steady state, the voltage of the proposed control strategy is closer to the target voltage of 220V, and the steady state error is smaller. This can be attributed to the FNN's approximation of the unknown parameters and errors of the system, which makes the control system more accurate. Fig.7 represents the current waveform under the two control methods. They all have a stable current, and the larger pulse current is suppressed by the inductor when the rectifier load is connected.

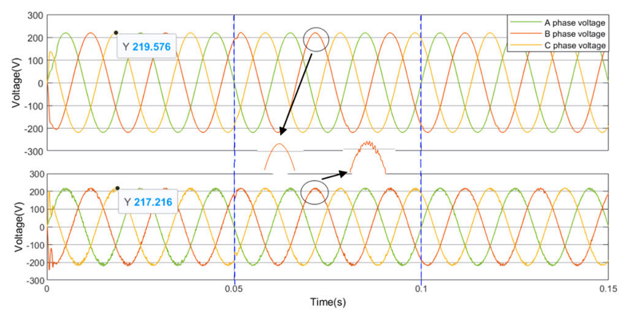

FIGURE 6. Voltage when connected to the rectified load under the proposed controller and traditional controller.

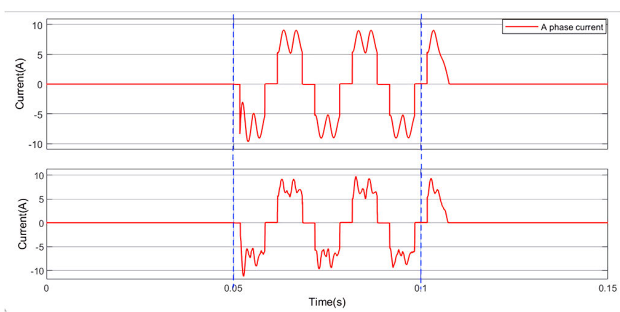

FIGURE 7. Current when connected to the rectified load under the proposed controller and traditional controller.

Fig.8 and Fig.9 represent the voltage harmonic content at different moments under different control strategies. After the voltage reaches stability at t=0.02, the voltage harmonics under the proposed control strategy are 0.32% and the voltage amplitude is 219.4V, which is less harmonic and steady-state error than the traditional control method. It can be seen in Fig. 8(b) and Fig.9(b), at t=0.5s, the voltage under the proposed control strategy has a small fluctuation due to the

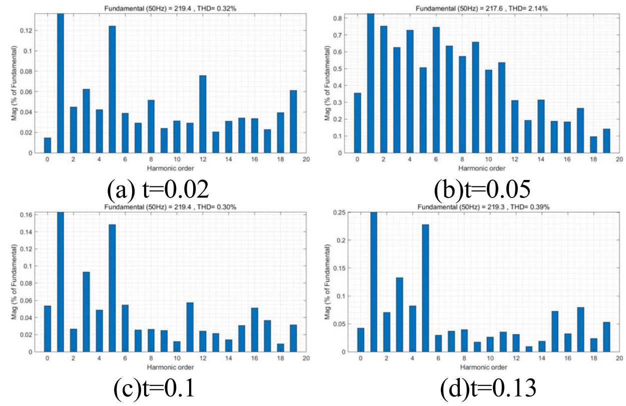

FIGURE 8. Harmonic content when connected to rectified mental loads under the proposed controller.

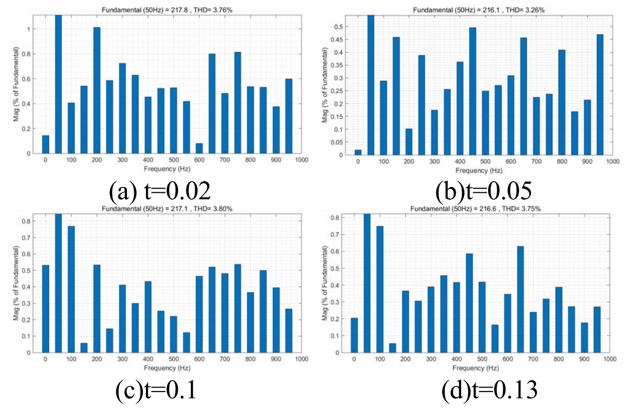

FIGURE 9. Harmonic content when connected to rectified mental loads under the traditional controller.

access of rectifying load but still has a good performance. Fig.8(c) and Fig.9(c) show that after the voltage stabilizes again, at t=0.1s, the rectifier load is removed, at which time the voltage amplitude and harmonics remain stable. Fig.8(d) and Fig.9(d) represent the voltage amplitudes of 219.3V and 216.6V with harmonic content of 0.39% and 3.75% for the two control strategies after voltage stabilization at t = 0.13s.

The FNN system shows a strong learning ability and generalization ability in the process of fitting approximation to the parameters for the system.

B. HARDWARE IN THE LOOP EXPERIMENTAL

In the past 20 years, DSP technology has been widely used in various fields. It is more accurate, flexible, smaller, and easier to integrate on a large scale than analog signal processors. However, the difficulty of implementing complex intelligent algorithms leads researchers to spend extra time on hardware, which is not conducive to algorithm tuning and optimization.

The dSPACE Real-Time system is a convenient and efficient platform for experiments and simulations based on Matlab/Simulink. Compared with DSP, it has a faster calculation speed and simpler operation. Meanwhile, it can be compiled and debugged by Matlab/Simulink, which significantly reduces the algorithm improvement time. In this paper, the DS1202 is used to design an experimental prototype to verify the practical effect of the proposed method. Considering the limitations of the conditions, the experimental prototype builds a low-voltage(24V/50HZ) three-phase UPS inverter for safety. The entire experimental session consists of the following three steps:

1) Simulation model creation and offline simulation in MATLAB. The model created is similar to the previous section, but with different voltages and resistant loads

2) The Real-time integration(RTI) library is the connection toolbox that comes with dSPACE. Select the appropriate I/O module to link with the simulation model and compile it into code that the DS1202 can execute.

3) After the download of the program to the DS1202, it is possible to monitor the system data and adjust the relevant parameters online through the Controldesk software.

Fig.10 shows the photograph of the experimental setup. At the moment t=0, the UPS works in inverter mode and starts up with unloading. At the moment of t=0.899s 30w load is added, at the moment of t=2.379s adding another 30w load.

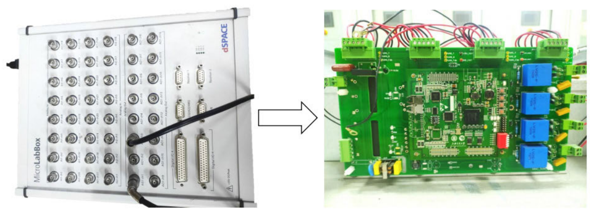

FIGURE 10. Photograph of the experimental setup.

Fig.11 shows the change in voltage and current when the load changes from unloading to half load. Fig.12 shows the change in voltage and current when the load changes from half load to full load.

When the load changes, the voltage can remain stable and reach the target voltage. Meet the basic requirements of UPS inverters. The current changes smoothly and the load has little impact on the UPS inverter. The good performance of the backstepping control for nonlinear systems is demonstrated. The perturbations during the experiment are suppressed by the sliding mode gain, which also reflects the powerful learning ability of the neural network.

Fig.13 reflects the output power when the load varies. The output power can quickly meet the load demand, which shows that the proposed control strategy has good reflection speed under the condition that the power input is sufficient.

The voltage and current waveforms measured under the MDO4034B-3 series oscilloscope are shown in Fig.14.

From experimental results, it can be seen that the UPS has good adaptability at different power levels with the proposed control strategy. The controller design requires fewer parameters compared to the general UPS backstepping control

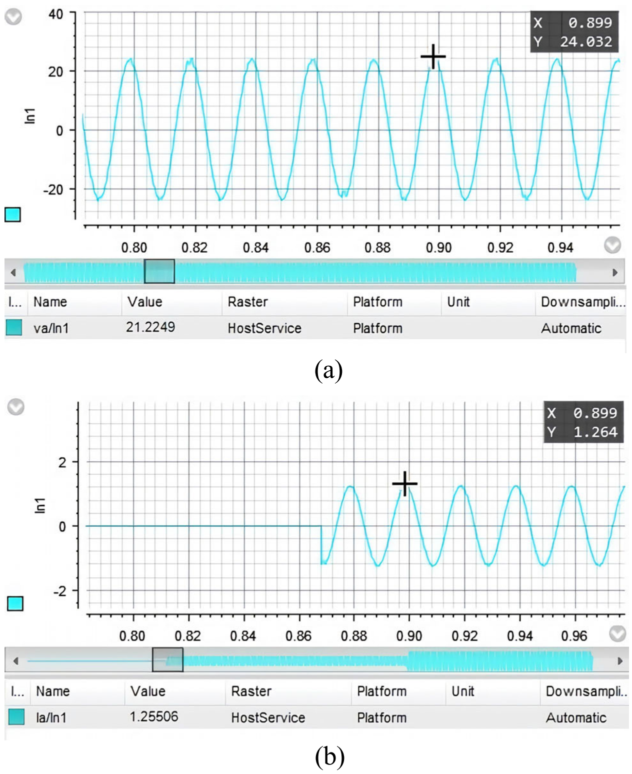

FIGURE 11. Voltage(a) and current(b) variation with load change.

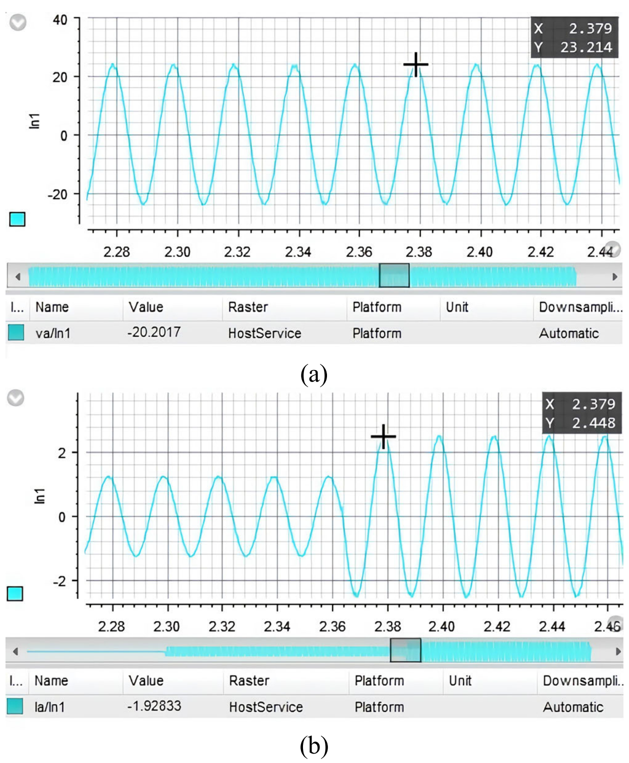

FIGURE 12. Voltage(a) and current(b) variation with load change.

method. Using FNN to approximate the unknown currents and disturbances, the controller shows excellent tracking performance in all stages.

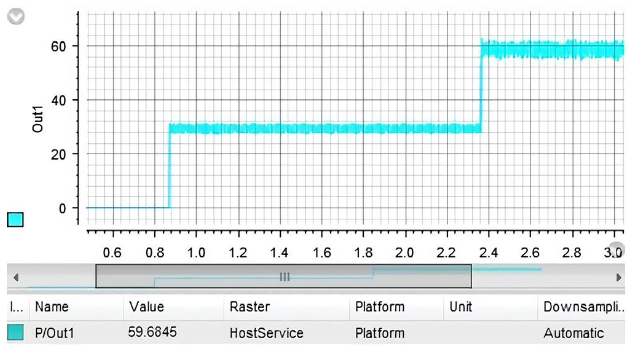

FIGURE 13. Output power waveform.

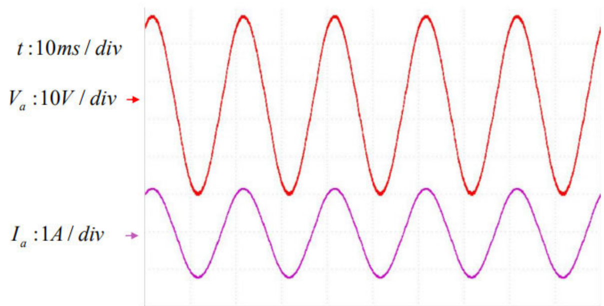

FIGURE 14. Voltage and current waveforms at stabilization.

V. CONCLUSION

In this paper, a novel control strategy for UPS inverters is proposed by using a combination of backstepping control and fuzzy neural networks. Compared to general control methods, only a small number of system parameters and a simple design are required, thus saving hardware measurement costs. The universal approximation property of FNN for unknown nonlinear functions is utilized to approximate the unknown system parameters and perturbation errors. A sliding mode component is incorporated into the controller design to improve the robustness of the system in the face of various perturbations. The effectiveness of the control method is verified by the dSPACE experimental platform, and the performance is still kept excellent in the face of multiple load variations. In the future, we are extending the proposed control strategy to the parallel connection of multi-level UPS.

REFERENCES

[1] T. Dragicevic and M. Novak, "Weighting factor design in model predictive control of power electronic converters: An artificial neural network approach," *IEEE Trans. Ind. Electron.*, vol. 66, no. 11, pp. 8870–8880, Nov. 2019.

[2] M. Bao-Kun, G. Li-Yuan, T. Xiao-Xu, C. Jin-pei, and Y. Xi-Ming, "Application of photovoltaic uninterruptible power supply system in distribution network communication station," in *Proc. China Int. Conf. Electr. Distrib. (CICED)*, Sep. 2018, pp. 101–105.

[3] S. S. H. Bukhari, T. A. Lipo, and B.-I. Kwon, "An online UPS system that eliminates the inrush current phenomenon while feeding multiple load transformers," *IEEE Trans. Ind. Appl.*, vol. 53, no. 2, pp. 1149–1156, Mar. 2017.

[4] M. Müller, N. Kimiaie, and A. Glüsen, "Direct methanol fuel cell systems for backup power—Influence of the standby procedure on the lifetime," *Int. J. Hydrogen Energy*, vol. 39, no. 36, pp. 21739–21745, Dec. 2014.

[5] S. S. H. Bukhari and J.-S. Ro, "A single-phase line-interactive UPS system for transformer-coupled loading conditions," *IEEE Access*, vol. 8, pp. 23143–23153, 2020.

[6] F. Zhu, Z. Peng, W. Hu, H. Wang, C. Zhang, Z. Zhao, and Y. Dai, "An improved VSG control strategy for microgrid," in *Proc. IEEE Int. Conf. Electr. Eng. Mechatronics Technol. (ICEEMT)*, Jul. 2021, pp. 338–342.

[7] W. Jian, L. Tong, L. ZiDong, and X. DianGuo, "VSG current balance control strategy under unbalanced grid voltage," in *Proc. 22nd Int. Conf. Electr. Mach. Syst. (ICEMS)*, Aug. 2019, pp. 1–6.

[8] K. Wali, R. Koubaa, and L. Krichen, "Voltage drop control for V2G applications," in *Proc. 16th Int. Multi-Conf. Syst., Signals Evices (SSD)*, Mar. 2019, pp. 40–43.

[9] M. Zhu, W. Li, X. Liang, S. Xu, B. Zhou, and Y. Shen, "Stepwise voltage drop and transient current control strategies to enhance fault ride-through capability of MMC-HVDC connected DFIG wind farms," *IEEE Trans. Power Syst.*, vol. 36, no. 3, pp. 2127–2137, May 2021.

[10] X. Meng, J. Liu, and Z. Liu, "A generalized droop control for grid-supporting inverter based on comparison between traditional droop control and virtual synchronous generator control," *IEEE Trans. Power Electron.*, vol. 34, no. 6, pp. 5416–5438, Jun. 2019.

[11] H. Katir, A. Abouloifa, K. Noussi, and I. Lachkar, "Adaptive backstepping control of cascaded H-Bridge multilevel DC/AC converters," in *Proc. 4th World Conf. Complex Syst. (WCCS)*, Apr. 2019, pp. 1–6.

[12] H. Katir, A. Abouloifa, K. Noussi, I. Lachkar, and F. Giri, "Cascaded H-bridge inverters for UPS applications: Adaptive backstepping control and formal stability analysis," in *Proc. Amer. Control Conf. (ACC)*, May 2021, pp. 2455–2460.

[13] Y. Wang and R.-J. Wai, "Design of discrete-time backstepping sliding-mode control for LCL-type grid-connected inverter," *IEEE Access*, vol. 8, pp. 95082–95098, 2020.

[14] K. Ali, Q. Khan, S. Ullah, I. Khan, and L. Khan, "Nonlinear robust integral backstepping based MPPT control for stand-alone photovoltaic system," *PLoS ONE*, vol. 15, no. 5, May 2020, Art. no. e0231749.

[15] H. Yang and D. Ye, "Adaptive fuzzy nonsingular fixed-time control for nonstrict-feedback constrained nonlinear multiagent systems with input saturation," *IEEE Trans. Fuzzy Syst.* vol. 29, no. 10, pp. 3142–3153, Oct. 2021.

[16] F. Wang, B. Chen, C. Lin, J. Zhang, and X. Meng, "Adaptive neural network finite-time output feedback control of quantized nonlinear systems," *IEEE Trans. Cybern.*, vol. 48, no. 6, pp. 1839–1848, Jun. 2018.

[17] S. Xu, C. Li, Y. Wang, and B. Li, "A low voltage single phase online uninterruptible power supply system based on APFC and fuzzy PID algorithm," *IEEE Access*, vol. 9, pp. 162389–162400, 2021.

[18] M. Kelemen, V. Polishchuk, B. Gavurová, S. Szabo, R. Rozenberg, M. Gera, J. Kozuba, R. Andoga, A. Divoková, and P. Blištan, "Fuzzy model for quantitative assessment of environmental start-up projects in air transport," *Int. J. Environ. Res. Public Health*, vol. 16, no. 19, p. 3585, 2019.

[19] J. W. Jung, V. Q. Leu, D. Q. Dang, T. D. Do, F. Mwasilu, and H. H. Choi, "Intelligent voltage control strategy for three-phase UPS inverters with output LC filter," *Int. J. Electron.*, vol. 102, no. 8, pp. 1267–1288, Aug. 2015.

[20] K. Zheng, Q. Zhang, Y. Hu, and B. Wu, "Design of fuzzy system-fuzzy neural network-backstepping control for complex robot system," *Inf. Sci.*, vol. 546, pp. 1230–1255, Feb. 2021.

[21] Y.-G. Kwak, D.-H. Heo, S.-P. Kim, S.-G. Song, S.-J. Park, and F.-S. Kang, "Reliability and economic efficiency analysis of 4-leg inverter compared with 3-leg inverters," *Electronics*, vol. 10, no. 1, p. 87, Jan. 2021.

[22] T. Ascensão and A. Jamshidnejad, "Autonomous socially assistive drones performing personalized dance movement therapy: An adaptive fuzzy-logic-based control approach for interaction with humans," *IEEE Access*, vol. 10, pp. 15746–15770, 2022.

[23] C.-H. Lien, H.-C. Chang, K.-W. Yu, H.-C. Li, and Y.-Y. Hou, "Robust mixed performance control of uncertain T-S fuzzy systems with interval time-varying delay by sampled-data input," *IEEE Access*, vol. 10, pp. 28109–28121, 2022.

[24] M. F. Khan, A. Haq, A. Ahmed, and I. Ali, "Multiobjective multi-product production planning problem using intuitionistic and neutrosophic fuzzy programming," *IEEE Access*, vol. 9, pp. 37466–37486, 2021.

[25] Y. Han, G. He, X. Fan, Q. Zhao, and H. Shen, "Design and analysis of improved ADRC controller for multiple grid-connected photovoltaic inverters," *Mod. Phys. Lett. B*, vol. 32, no. 34n36, Dec. 2018, Art. no. 1740103.

[26] H. Y. Wang, J. S. Wang, and G. Wang, "Combination evaluation method of fuzzy C-mean clustering validity based on hybrid weighted strategy," *IEEE Access*, vol. 9, pp. 27239–27261, 2021.

[27] X. Dang, X. Zhao, C. Dang, H. Jiang, X. Wu, and L. Zha, "Incomplete differentiation-based improved adaptive backstepping integral sliding mode control for position control of hydraulic system," *ISA Trans.*, vol. 109, pp. 199–217, Mar. 2021.

[28] J. Ma, J. H. Park, and S. Xu, "Command-filter-based finite-time adaptive control for nonlinear systems with quantized input," *IEEE Trans. Autom. Control*, vol. 66, no. 5, pp. 2339–2344, May 2021.

YANFEI DONG received the B.S. degree in mechanical and electrical integration from the Zhengzhou Antiaircraft Artillery College, Henan, China, in 1999, and the M.S. degree in electrical engineering from Wuhan University, Hubei. His research interests include motor control and power equipment diagnosis.

GUOYONG ZHANG received the B.S. degree in electrical engineering and automation from the Sichuan University of Science and Engineering, Sichuan, China, in 2016.

GUOFENG HE received the B.S. degree in mechanical and electronic engineering from the Luoyang Institute of Technology, Luoyang, China, in 1996, the M.S. degree in electrical engineering from Shandong University, Shandong, China, in 2004, and the Ph.D. degree in power electronics from Zhejiang University, Hangzhou, China, in 2014. He worked as a Master's Supervisor of China Three Gorges University, in 2021. He is currently a Professor with the Henan University of Urban Construction. His research interests include digital control of parallel UPS systems, high-frequency high-power conversion, and renewable energy power conversion systems.

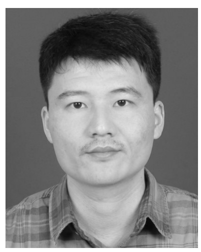

WENJIE SI received the B.S. and M.S. degrees in control theory and control engineering from Zhengzhou University, Zhengzhou, China, in 2008 and 2011, respectively, and the Ph.D. degree in control theory and control engineering from the South China University of Technology, Guangzhou, China, in 2015. He was an Assistant Professor with the School of Automation Science and Engineering, South China University of Technology.